

# Effects of micro-fluctuations on magnetic island evolution

S. Nishimura<sup>1)</sup>, S. Benkadda<sup>1)</sup>, M. Yagi<sup>1)</sup>, S.-I. Itoh<sup>1)</sup> and K. Itoh<sup>1)</sup>

<sup>1)</sup>France-Japan Magnetic Fusion Laboratory LIA 336, Université de Provence-CNRS/UMR6633, 13397 Marseille, France

<sup>2)</sup>Interdisciplinary Graduate School of Engineering Sciences, Kyushu University, Fukuoka 816-8580, Japan

<sup>3)</sup>Equipe DSC, Laboratoire PIIM, UMR 6633 CNRS-Université de Provence, 13397 Marseille, France

<sup>4)</sup>Research Institute for Applied Mechanics, Kyushu University, Fukuoka 816-8580, Japan

<sup>5)</sup>National Institute of Fusion Science, Gifu 509-5292, Japan

(Received: 29 August 2008 / Accepted: 15 December 2008)

The coexistence of the drift-tearing mode and the resistive drift-interchange mode is numerically simulated using a reduced set of two-fluid equations, in order to investigate effects of micro-fluctuations and the zonal flow on the magnetic island dynamics. It is found that the growth rate of the magnetic island is nonlinearly accelerated by micro-fluctuations generated by the resistive drift-interchange mode. The rotation frequency of the magnetic island in the nonlinear phase is dominated by the zonal flow mainly generated by Reynolds stress and Maxwell stress associated with the magnetic island. Micro-fluctuations indirectly affect the excitation of the zonal flow by modifying the radial structure of the magnetic island perturbation, which changes contributions of these stresses.

Keywords: magnetic island, micro-fluctuation, zonal flow, nonlinear interaction

## 1. Introduction

The magnetic island is often observed in the magnetically confined fusion plasmas such as tokamak plasmas and other laboratory plasmas. The excitation of magnetic islands is associated with the reconnection of the magnetic field line, where the perturbation perpendicular to the ambient magnetic field grows to the large scale. The consequent change of the topology of the magnetic field affects the confinement and the stability of plasmas. Much works have been done for the stability of magnetic islands, and it has been pointed out that the small magnetic island is stable from view point of the linear stability analysis. Nowadays, the mechanism of the excitation of magnetic islands is discussed, based on the nonlinear instability associated with the bootstrap current. However, the seeding process, which triggers the excitation of magnetic islands, is still an unsolved problem, and many candidates have been suggested[1, 2]. Especially, the rotation of magnetic islands is an important factor for the sub-critical excitation of magnetic islands via the polarization current[3]. Simultaneously, the hierarchical interaction between the magnetic island and the background turbulence should be clarified. In fact, the stochastic excitation of magnetic islands by the background turbulence has been pointed out in both the analytical theory[4, 5] and the numerical simulation[6].

The purpose of this study is to examine the basic mechanism of the influence of micro-fluctuations and the zonal flow on the growth rate and the rotation frequency of the magnetic island. To this aim, we introduce a simple model including so-called the

drift-tearing mode (DTM), which is the linearly unstable tearing mode combined with the electron density and temperature[7]. Moreover, micro-fluctuations are mainly generated by the resistive interchange mode in our model, which is destabilized by the curvature of the magnetic field line.

## 2. Model equation

In this study, large aspect ratio tokamak plasmas ( $\epsilon = a/R_0 \ll 1$ , where  $\epsilon$ ,  $a$  and  $R_0$  are the inverse aspect ratio, the minor and the major radii, respectively) are considered. We introduce a reduced set of two-fluid equations derived from Braginskii's two-fluid equations[8]. Renormalizing the curvature of the magnetic field line, the simple cylindrical coordinate  $(r, \theta, z)$  is considered, where variables represent the radial position, poloidal angle and toroidal position, respectively. The model equations are

$$\frac{D}{Dt} \nabla_{\perp}^2 \phi = \nabla_{\parallel} j_{\parallel} - [\Omega, p] + \mu \nabla_{\perp}^4 \phi, \quad (1)$$

$$\frac{\partial}{\partial t} A = -\nabla_{\parallel} (\phi - \delta p) - \eta_{\parallel} j_{\parallel} + \alpha_T \delta \nabla_{\parallel} T, \quad (2)$$

$$\frac{D}{Dt} n + \beta \frac{D}{Dt} p = \delta \beta \nabla_{\parallel} j_{\parallel} + \beta [\Omega, \phi - p] + \eta_{\perp} \beta \nabla_{\perp}^2 p, \quad (3)$$

$$\frac{3}{2} \frac{D}{Dt} T - \frac{D}{Dt} n = \alpha_T \delta \beta \nabla_{\parallel} j_{\parallel} + \epsilon^2 \chi_{\parallel} \nabla_{\parallel}^2 T + \chi_{\perp} \nabla_{\perp}^2 T, \quad (4)$$

where  $j_{\parallel} = -\nabla_{\perp}^2 A$ ,  $\alpha_T = 0.71$ ,  $D/Dt = \partial/\partial t + [\phi, ]$ ,  $\nabla_{\parallel} = \partial/\partial z - [A, ]$ ,  $\nabla_{\perp} = \hat{\mathbf{r}}\partial/\partial r + \hat{\boldsymbol{\theta}}(1/r)\partial/\partial\theta$  and  $[f, h] = \hat{\mathbf{z}} \cdot \nabla f \times \nabla h$ .  $\{\hat{\mathbf{r}}, \hat{\boldsymbol{\theta}}, \hat{\mathbf{z}}\}$  indicate unit vectors.  $\nabla\Omega$  is a curvature of the magnetic field line defined by

author's e-mail: nseiya@riam.kyushu-u.ac.jp

$\nabla\Omega = -(\hat{\mathbf{b}} \cdot \nabla)\hat{\mathbf{b}}$ , where  $\hat{\mathbf{b}}$  is a unit vector along the magnetic field line. We apply the concentric curvature such that  $\nabla\Omega = g\hat{\mathbf{r}}$ , where  $g$  is assumed to be constant for simplicity. For example, the term  $[\Omega, p]$  in Eq.(1) is given by

$$[\Omega, p] = g \frac{1}{r} \frac{\partial p}{\partial \theta}.$$

$\{\phi, A, n, T, p\}$  indicate electrostatic potential, vector potential parallel to the ambient magnetic field, electron density, electron temperature and electron pressure defined by  $p = n + T$ , respectively.  $\{\mu, \eta_{\parallel}, \eta_{\perp}, \chi_{\parallel}, \chi_{\perp}\}$  are ion viscosity, parallel resistivity, perpendicular resistivity, parallel and perpendicular thermal conductivity, respectively.  $\{\delta, \beta\}$  indicate ion skin depth normalized by the minor radius and the plasma beta value, respectively. The normalization is  $\{v_A t/R_0 \rightarrow t, r/a \rightarrow r, z/R_0 \rightarrow z\}$ , where  $v_A$  is Alfvén velocity. The total energy defined by

$$E = \frac{1}{2} \int |\nabla_{\perp} \phi|^2 dV + \frac{1}{2} \int |\nabla_{\perp} A|^2 dV + \frac{1}{2\beta} \int |n|^2 dV + \frac{3}{4\beta} \int |T|^2 dV + \frac{1}{2} \int |p|^2 dV,$$

is conserved in the dissipationless limit, where  $\int dV$  indicates the volume integral. Each perturbed quantity  $f(r, \theta, z, t)$  is assumed to vary as

$$f_0(r) + \sum_{m,n} \tilde{f}_{m,n}(r, t) \exp\{i(m\theta - nz)\},$$

where  $m$  and  $n$  are the poloidal and toroidal mode number. The perturbation  $\tilde{f}_{m,n}(r)$  satisfies boundary conditions:  $\tilde{f}_{m,n}(0) = \tilde{f}_{m,n}(1) = 0$  for  $m, n \neq 0$  and  $\partial\tilde{f}_{0,0}/\partial r|_{r=0} = \tilde{f}_{0,0}(1) = 0$  (the center and edge of plasma correspond to  $r = 0$  and  $r = 1$ ). The equilibrium quantities are chosen such that

$$\begin{aligned} q(r) &= 1.5 + 0.5 \left( \frac{r}{r_s} \right)^3, \\ n'_0 &= -\frac{2\beta}{\epsilon} r, \\ T'_0 &= -\frac{2\beta}{\epsilon} r, \end{aligned}$$

where  $q(r)$  stands for the safety factor defined by  $1/q(r) = -(1/r)A'_0$ ,  $r_s$  is the radial position of the rational surface and the prime indicates the radial derivative. The equilibrium current  $j_0(r)$  is given by the cylindrical magnetohydrodynamic (MHD) equilibrium with the equilibrium pressure. We set  $r_s = 0.6$ ,  $\epsilon = 0.2$ ,  $\beta = 0.01$  and  $\delta = 0.01$ , and  $g$  is set to be 0 or 0.09. Transport coefficients are chosen as  $\mu = 10^{-5}$ ,  $\eta_{\parallel} = 10^{-5}$ ,  $\eta_{\perp} = 2 \times 10^{-5}$ ,  $\chi_{\parallel} = 1$  and  $\chi_{\perp} = 10^{-5}$ . Note that a ratio  $\chi_{\parallel}/\chi_{\perp}$  is crucial for excitation of the neoclassical tearing mode, but not for the drift-tearing mode[8]. For this reason, we use

a small value of  $\chi_{\parallel}$  to save the simulation time. In this study, we adopt a predictor-corrector scheme to calculate time evolutions, and a spectral method to evaluate nonlinear terms, where only modes, which satisfy  $m/n = 2$  (resonant modes on the  $q = 2$  surface), is considered, for simplicity. The radial grid has 512 meshes, and the time step is 0.01. In the following nonlinear simulation, sixteen harmonics and the quasi-linear modification of equilibrium fields, i.e.  $(m, n) = (2, 1), (4, 2), \dots, (32, 16)$  and  $(0, 0)$  and their complex conjugates, are included. The simulation with a single harmonics,  $(m, n) = (2, 1)$  and  $(0, 0)$  is also examined as the reference case (hereafter, we simply mention the case without higher harmonics).

The set of Eq.(1) and (2) with  $\delta = g = 0$  describes the classical tearing mode. The finite  $\delta$  combines the tearing mode with the electron density and temperature, in other words the effect of the electron diamagnetic drift. In addition, this instability is categorized into the so-called collisional DTM in the present parameter regime[7]. The resistive drift-interchange mode (DIM) is driven by the finite curvature  $g$ [9].

We introduce the analytical formula of the rotation frequency of the magnetic island for the following analysis. Using the  $(2, 1)$  component of Eq.(2), and assuming that it is proportional to  $e^{-i\omega t}$ , where  $\text{Im}(\omega)$  and  $\text{Re}(\omega)$  are the growth rate and the rotation frequency of magnetic island, we obtain

$$\text{Re}(\omega) \approx \langle \omega_* + \tilde{\omega}_* \rangle + \langle \tilde{\omega}_{E \times B} \rangle + \text{Re} \langle L_{\eta_{\parallel}} \rangle + \text{Re} \langle L_{k_{\parallel}} \rangle, \quad (5)$$

where the bracket  $\langle \rangle$  indicates the radial average inside magnetic islands at each time step. Variables in Eq.(5) are defined by  $\omega_* + \tilde{\omega}_* = -\delta k_{\theta_{2,1}} [n'_0 + \tilde{n}'_{0,0} + (1 + \alpha_T)(T'_0 + \tilde{T}'_{0,0})]$ ,  $\tilde{\omega}_{E \times B} = k_{\theta_{2,1}} \tilde{\phi}'_{0,0}$ ,  $L_{\eta_{\parallel}} = i\eta_{\parallel} \nabla_{\perp}^2 \tilde{A}_{2,1} / \tilde{A}_{2,1}$  and  $L_{k_{\parallel}} = k_{\parallel_{2,1}} [\tilde{\phi}_{2,1} - \delta \{ \tilde{n}_{2,1} + (1 + \alpha_T) \tilde{T}_{2,1} \}] / \tilde{A}_{2,1}$ , respectively, where  $k_{\theta_{m,n}} = m/r$ ,  $k_{\parallel_{m,n}} = m(1/q + 1/\tilde{q}) - n$  and  $1/\tilde{q} = -(1/r) \tilde{A}'_{0,0}$ . The first and the second terms in Eq.(5) indicate contributions from the electron diamagnetic drift and the zonal flow, respectively. The third and the forth terms arise from the resistivity and the dynamics along the magnetic field line. When we have the electromagnetic perturbation, the zonal flow is generated by not only Reynolds stress but also Maxwell stress. The analytical formula of the zonal flow contribution  $\langle \tilde{\omega}_{E \times B} \rangle$  is derived from the  $(0, 0)$  component of Eq.(1) such that

$$\langle \tilde{\omega}_{E \times B} \rangle = \left\langle \int^t R dt' \right\rangle + \left\langle \int^t M dt' \right\rangle + \left\langle \int^t V dt' \right\rangle, \quad (6)$$

where the first, the second and the third terms indicate contributions of Reynolds stress, Maxwell

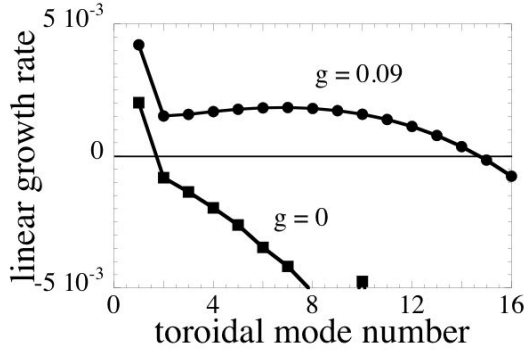


Fig. 1 The linear growth rate spectrum of the toroidal mode number.

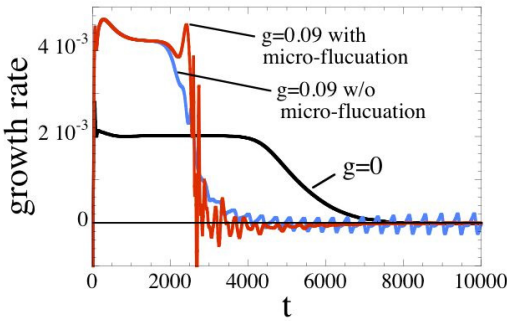


Fig. 2 The time evolution of the growth rate of the magnetic island.

stress and the ion viscosity, respectively. Variables are defined by  $R = -(k_{\theta_{2,1}}/r) \int^r dr r[\tilde{\phi}, \nabla_{\perp}^2 \tilde{\phi}]_{0,0}$ ,  $M = (k_{\theta_{2,1}}/r) \int^r dr r[\tilde{A}, \nabla_{\perp}^2 \tilde{A}]_{0,0}$ ,  $V = \mu k_{\theta_{2,1}} \times (\partial/\partial r) \{(1/r)(\partial/\partial r)(r\tilde{\phi}'_{0,0})\}$ , where  $[f, g]_{0,0}$  indicate the summation of  $(0, 0)$  Fourier components by the nonlinear coupling of modes. Note that the curvature  $g$  does not included in Eq.(6) explicitly, i.e. the curvature indirectly affects the zonal flow via the modification of the mode structure of perturbations, which modifies the characteristics of Reynolds stress and Maxwell stress.

### 3. Analysis

Figure 1 shows the linear growth rate with the toroidal mode number. Two cases are plotted:  $g = 0$  and  $g = 0.09$ , where the linear growth rate of the DTM corresponds to the lowest mode number. In the case with  $g$ , the enhancement of the DTM and the resistive DIM in the higher harmonics are observed. The growth rate of the lowest mode number is larger than those of the higher harmonics. We confirmed that this situation is independent of values of  $g$  and  $\delta$  in the present parameter regime of interest.

Figure 2 shows the time evolution of the growth

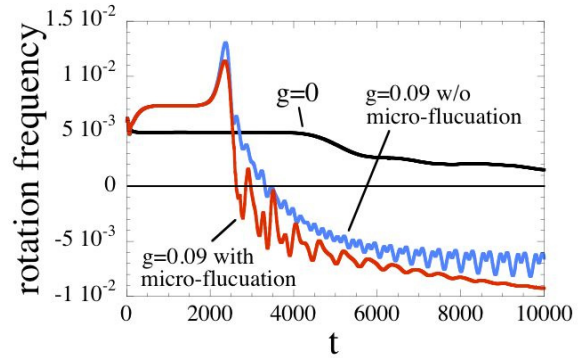


Fig. 3 The time evolution of the rotation frequency of the magnetic island.

rate of the magnetic island. For  $g = 0.09$ , two cases are plotted: the case with higher harmonics (micro-fluctuations), i.e.  $(4, 2), \dots, (32, 16)$ , and the case without them. Linear growth phases are observed in  $0 \leq t \leq 3800$  for the  $g = 0$  case,  $0 \leq t \leq 1800$  for the  $g = 0.09$  case, respectively, where growth rates in these phases are shown in Fig.1. Comparing  $g = 0.09$  cases, it is found that the growth of the magnetic island is nonlinearly accelerated by micro-fluctuations in  $2000 \leq t \leq 2500$ [10]. However, the saturation width of the magnetic island is not strongly affected by micro-fluctuation. This is because the saturation level of the magnetic island is mainly determined by the initial value of  $\Delta'$ .

Figure 3 shows the time evolution of the rotation frequency of the magnetic island. The positive and the negative signs indicate those of the electron diamagnetic drift and the ion diamagnetic drift directions, respectively. Three plots are obtained by the same nonlinear simulations in Fig.2. The rotation frequency in the linear phase is affected by the value of  $g$ , furthermore, the direction of the rotation frequency is reversed in the nonlinear regime.

In order to clarify the mechanism to change the direction of the rotation frequency by the curvature observed in Fig.3, the analytical formula of the rotation frequency Eq.(5) is used to decompose the rotation frequency into each pieces. Figure 4 shows time evolutions of each component of Eq.(5). We confirmed that the summation of these components successfully reproduces the result in Fig.3, except the high nonlinearity regime  $2000 \leq t \leq 2500$ . Note that vertical scales in these figures are not the same.  $\text{Re}\langle L_{\eta\parallel} \rangle$  in the nonlinear phase is negligible in each case. In comparison to Fig.4(a) and (c), the saturation value of  $\langle \omega_* + \tilde{\omega}_* \rangle$  in Fig.4(b) is reduced, i.e., the pressure gradient is strongly flattened. This is caused by the enhancement of the transport by micro-fluctuations. The different behavior of  $\text{Re}\langle L_{k\parallel} \rangle$  implies the modifi-

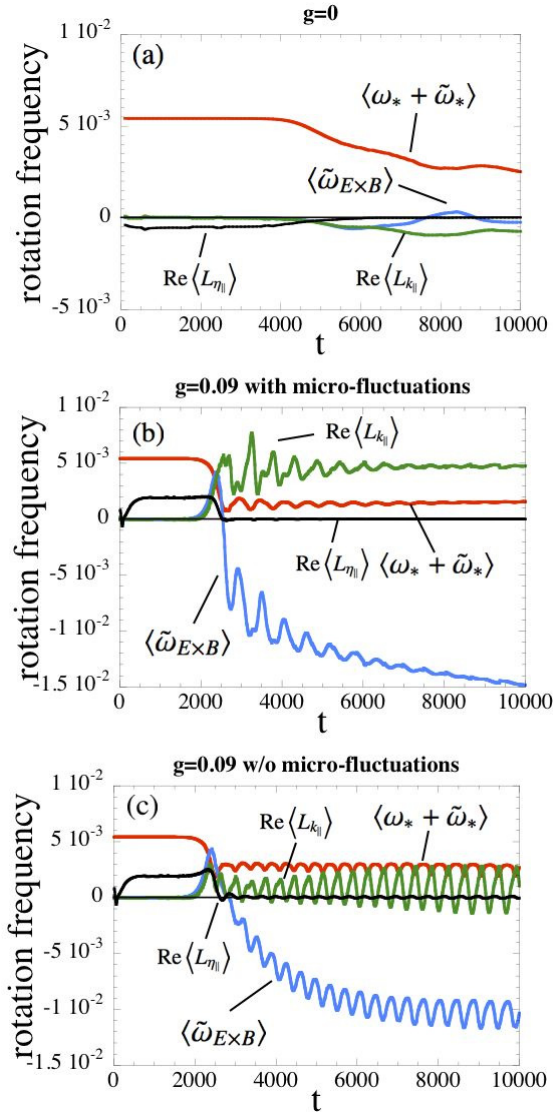


Fig. 4 The time evolution of components of the rotation frequency of the magnetic island: (a) the case with  $g = 0$ , (b) the case with  $g = 0.09$  including micro-fluctuations.

cation of the radial structure of the eigenfunction of the magnetic island. It is found that the reversal of the rotation frequency is mainly caused by the contribution of the zonal flow  $\langle \tilde{\omega}_{E \times B} \rangle$ . The change of the contribution of the zonal flow implies that the radial pattern of the zonal flow velocity inside the magnetic island is modified by the curvature.

Finally, the generation mechanism of zonal flow is analyzed. We introduce a ratio of Reynolds stress to Maxwell stress,  $\langle \int^t R dt' \rangle : \langle \int^t M dt' \rangle$ . These ratios at  $t = 10000$  in each simulation normalized by the initial diamagnetic drift frequency ( $\langle \omega_* \rangle_{t=0} = 5.4 \times 10^{-3}$ ) are given by (I)  $-5.8 : 5.9$  for the case  $g = 0$ , (II)  $-5.9 : -1.2$  for the case  $g = 0.09$  with micro-fluctuations and (III)  $-0.38 : -6.1$  for the case  $g = 0.09$  with-

out micro-fluctuations, respectively. Note that signs in these ratios match with original directions of rotation frequency. In the DTM ( $g = 0$ ), these stresses approximately cancel out each other, and the zonal flow is not strongly excited. In the present study, the curvature plays an important role to introduce the incomplete cancellation between Reynolds stress and Maxwell stress. Comparing (I) ( $g = 0$ ) with (III) ( $g = 0.09$  without micro-fluctuations), it is found that the finite curvature changes the direction of the contribution of stresses, which triggers the excitation of the zonal flow. This implies that the curvature affects the mode structure of the DTM. While, the direct contribution of micro-fluctuations is not strong in the generation of the zonal flow, in other words, the zonal flow is mainly generated by the quasi-linear effect of the DTM. However, comparing (II) and (III) ( $g = 0.09$ ), it is confirmed that micro-fluctuations also affect these stresses indirectly, by modifying the structure of the perturbation associated with the magnetic island. In spite of the similarity of contributions of zonal flow in Fig.4(b) and (c), the generation mechanism of the zonal flow is different.

In conclusion, effects of micro-fluctuations and zonal flow on the evolution of the magnetic island are investigated. The micro-fluctuation nonlinearly accelerates the growth rate of magnetic island. The zonal flow generated by quasi-linear effects dominates the rotation frequency of magnetic island. The curvature and micro-fluctuations affect the generation of zonal flow, due to the unbalance between Reynolds stress and Maxwell stress. The effect of the strong unstable micro-fluctuations should be examined in the future work.

- [1] R. J. Buttery, T. C. Hender, D. F. Howell, R. J. La Haye, O. Sauter, D. Testa and contributors to the EFDA-JET Workprogramme, Nucl. Fusion **43** (2003) 69.
- [2] H. Reimerdes, O. Sauter, T. Goodman, and A. Pochelon, Phys. Rev. Lett. **88** (2002) 105005.
- [3] A. I. Smolyakov, Plasma Phys. Control. Fusion **35** (1993) 657.
- [4] S.-I. Itoh, K. Itoh, and M. Yagi, Phys. Rev. Lett. **91** (2003) 045003.
- [5] S.-I. Itoh, K. Itoh, and M. Yagi, Plasma Phys. Control. Fusion **46** (2004) 123.
- [6] M. Yagi, S. Yoshida, S.-I. Itoh, H. Naitou, H. Nagahara, J.-N. Leboeuf, K. Itoh, T. Matsumoto, S. Tokuda, and M. Azumi, Nucl. Fusion **45** (2005) 900.
- [7] J. F. Drake, T. M. Antonsen, Jr., A. B. Hassam, and N. T. Gladd, Phys. Fluids **26** (1983) 2509.
- [8] S. Nishimura, S. Benkadda, M. Yagi, S.-I. Itoh, and K. Itoh, Phys. Plasmas **15** (2008) 092506.
- [9] H. Sugama, M. Wakatani, and A. Hasegawa, Phys. Fluids **31** (1988) 1601.
- [10] M. Yagi, S.-I. Itoh, K. Itoh, M. Azumi, P. H. Diamond, A. Fukuyama, and T. Hayashi, Plasma Fusion Res. **2** (2007) 025.